Supplementary Information

Abnormal decrease in Curie temperature in pseudohalide rare-earth double perovskite ferroelastics driven by lanthanide contraction

Meng-Jun Lin,[a] Jun-Ying Li,[a] Pei-Guo Liu,[a] Ya-Ting Zou,[a] Hao-Fei Ni,[a] Lei Pan,[a] Gele Teri,[a] Chang-Feng Wang,*[a] Da-Wei Fu,*[a] and Yi Zhang*[a]

[a] Institute for Science and Applications of Molecular Ferroelectrics, Key Laboratory of the Ministry of Education for Advanced Catalysis Materials, Zhejiang Normal University, Jinhua 321004, China.

E-mail: wang1215@zjnu.edu.cn; dawei@zjnu.edu.cn; yizhang1980@seu.edu.cn

Synthesis methods:

The reagents used in this work were commercially obtained and used without further purification. DMSOX (20 mmol, 1.86 g) was dissolved in water, and an equimolar HNO_3 solution (20 mmol, 1.85 g) was slowly added dropwise under cooling and stirring to obtain an aqueous solution of $(DMSOX)NO_3$. Colorless block crystals of $(DMSOX)_2LaCs(NO_3)_6$ were obtained by slow evaporation of an aqueous solution containing $(DMSOX)NO_3$ (6 mmol, 0.93 g), $CsNO_3$ (1.5 mmol, 0.29g), and $La(NO_3)_3 \cdot 6H_2O$ (3 mmol, 1.30 g) at room temperature after one week. The other five compounds were synthesized following the same method.

Materials and methods:

Powder X-ray diffraction measurements (PXRD): The experimental PXRD patterns of the six compounds were collected at room temperature on a Bruker Advance diffractometer, with a 2θ range of 5° to 50° and a step size of 0.02°. Their simulated PXRD patterns were extracted from the respective CIF files using Mercury software. Comparison of the experimental patterns with the simulated patterns confirmed the high phase purity of all six synthesized compounds.

Thermal measurements: Thermogravimetric analysis (TGA) was performed on a NETZSCH STA 440 synchronous thermal analyzer. Approximately 10 mg of the sample was weighed into an alumina crucible. The measurement was performed under a nitrogen atmosphere, with a heating rate of 5 K min^{-1} over a temperature range from 20 °C to 1000 °C.

Differential scanning calorimetry (DSC) measurements：Differential scanning calorimetry (DSC) measurements were performed on a NETZSCH DSC 3500 instrument. Approximately 10 mg of the sample was weighed into an aluminum crucible. The test was conducted under a nitrogen atmosphere at a heating/cooling rate of 20 K min^{-1} over the specified temperature range.

Dielectric measurements: Dielectric constant measurements were performed on a TH2828A impedance analyzer. First, the crystals were ground into powder and dried. Using the SSP-10A flat-plate press, an appropriate amount of the powder was pressed into a sheet of suitable thickness. Then,

the sheet was cut into an appropriate size, and copper conductive paste was uniformly coated on both sides. The sample was fixed to the electrodes using the copper conductive paste and copper wires. Finally, the electrodes were connected to the TH2828A impedance analyzer for dielectric constant measurements.

Single crystal X-ray diffraction: Single crystal X-ray diffraction data were received on a Bruker D8 APEX-III diffractometer using Mo-Kα radiation (λ = 0.71073 Å, 50 kV/40 mA) to determine the crystal structures of the six compounds in the ferroelastic phase and paraelastic phase. Suitable single crystals were selected under an optical microscope and placed on the diffractometer. Data processing and numerical absorption corrections were performed using the APEX-III software. Structure solution and refinement were carried out with the SHELXT and Olex2 software packages.

Thin film preparation and testing equipment: 200 mg of $(DMSOX)_2EuCs(NO_3)_6$ crystals were weighed and dissolved in 5 mL of water, and a few drops of HNO_3 were slowly added to obtain a clear mixed solution. The indium tin oxide (ITO)-coated glass substrates were cleaned by ultrasonication and treated with UV-ozone for 15 minutes. Subsequently, 60 μL of the above solution was pipetted onto the substrates, and a thin film was slowly grown on a hot stage preheated to 313 K. Finally, the prepared thin film was placed under a CX40P polarized light microscope to observe the temperature-dependent evolution of ferroelastic domains. The other five compounds were also prepared as thin films and tested following the same method.

Calculation formulas for Δ*S* and Δ*H*: The enthalpy and entropy changes associated with the reversible phase transitions of the six compounds were calculated using the Boltzmann equation. The corresponding results are summarized in Table S1.

$$\Delta S = R\ln N = \int_{T_2}^{T_1} \frac{Q}{T} \mathrm{d}T = \frac{\Delta H}{T_C}$$

UV-visible (UV-vis) spectrophotometry measurements: The UV-Vis absorption spectrum of $(DMSOX)_2EuCs(NO_3)_6$ was measured on an Agilent Cary 5000 spectrometer with a spectral scanning range of 200-800 nm.

Photoluminescence (PL) measurements: The excitation and emission spectra of $(DMSOX)_2EuCs(NO_3)_6$ were obtained on an Edinburgh FLS1000 spectrofluorometer, and the fluorescence lifetime and photoluminescence quantum yield were also determined.

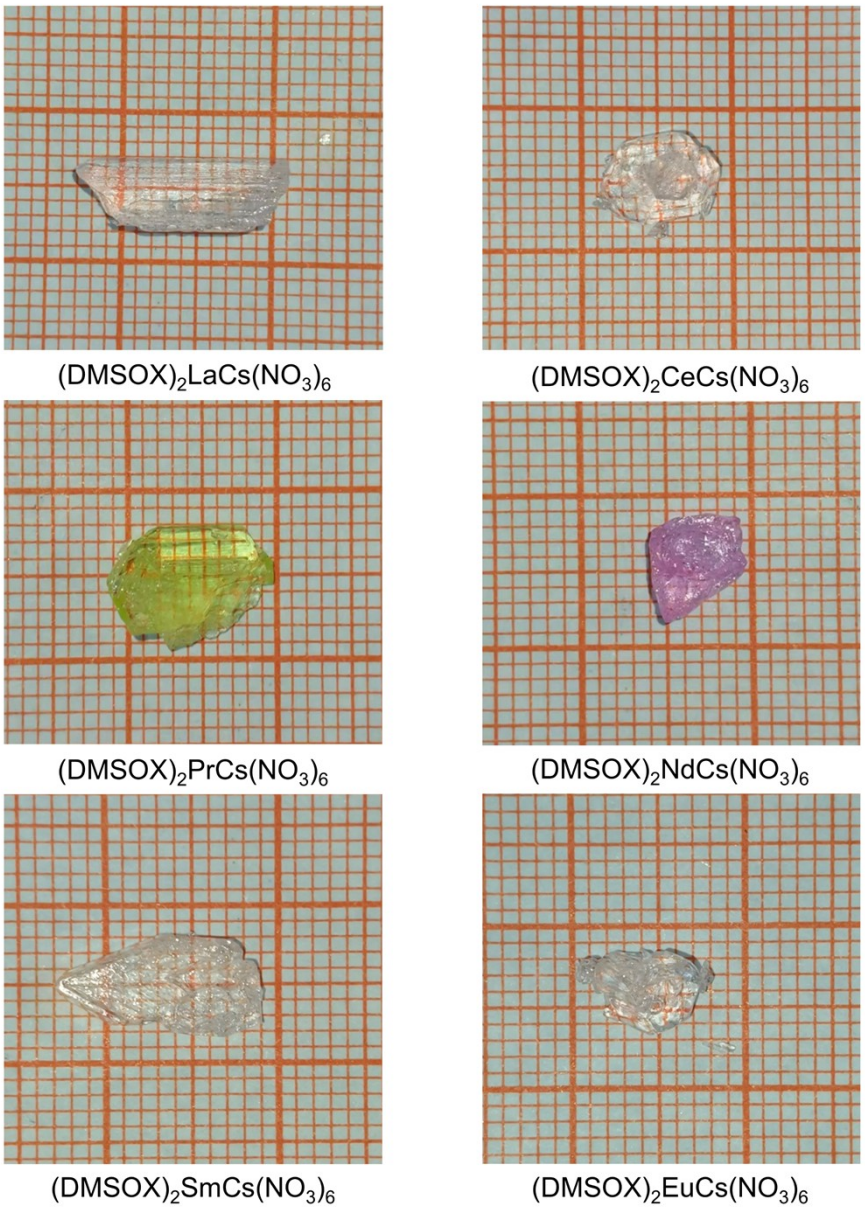

Fig. S1. Crystal morphology photos of $(DMSOX)_2LnCs(NO_3)_6$.

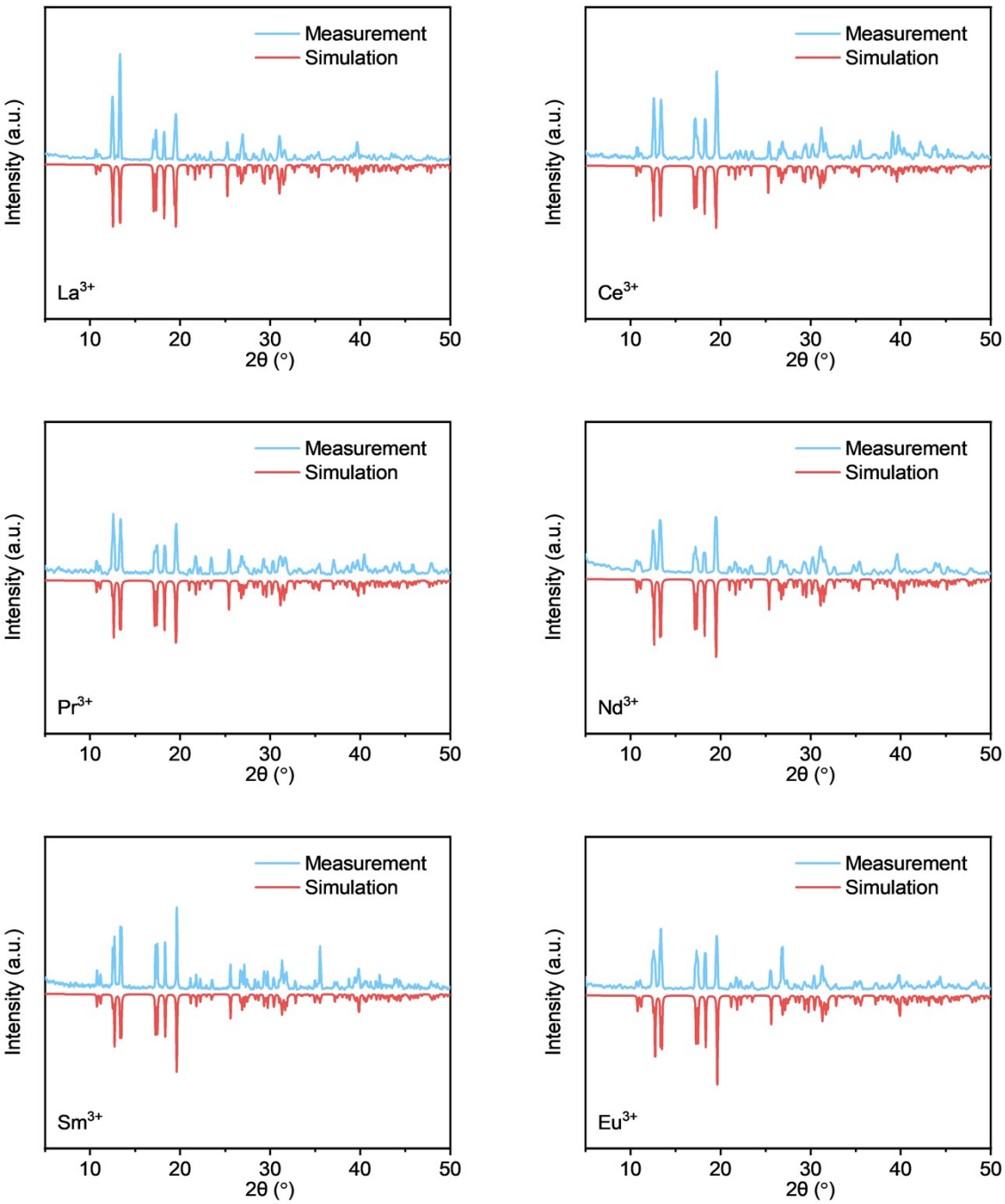

Fig. S2. Patterns of the PXRD for $(DMSOX)_2LnCs(NO_3)_6$. Where the blue line is the experimental result and the red line is simulated from the single crystal structure.

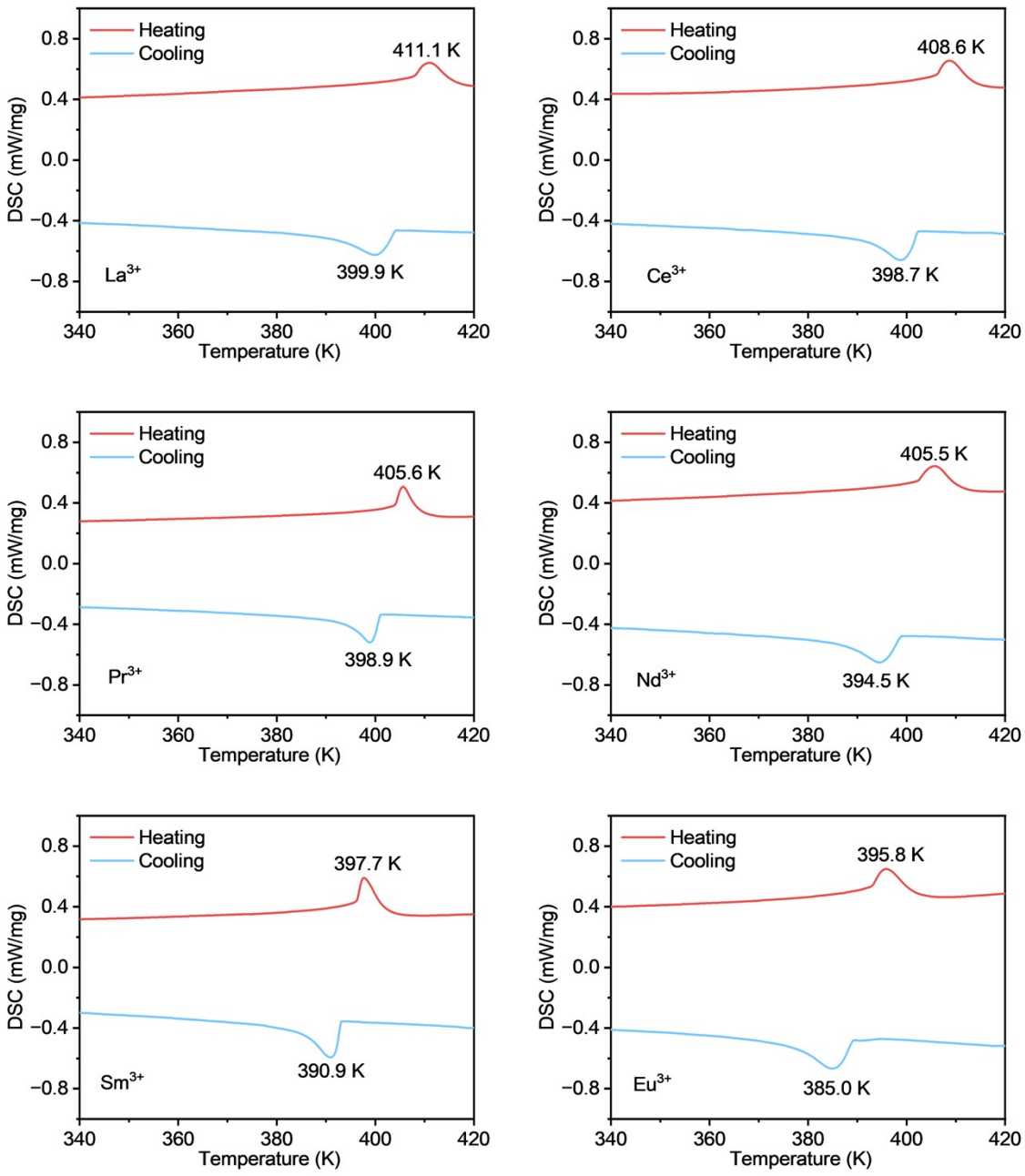

Fig. S3. The DSC curve for $(DMSOX)_2LnCs(NO_3)_6$ in a heating-cooling cycle.

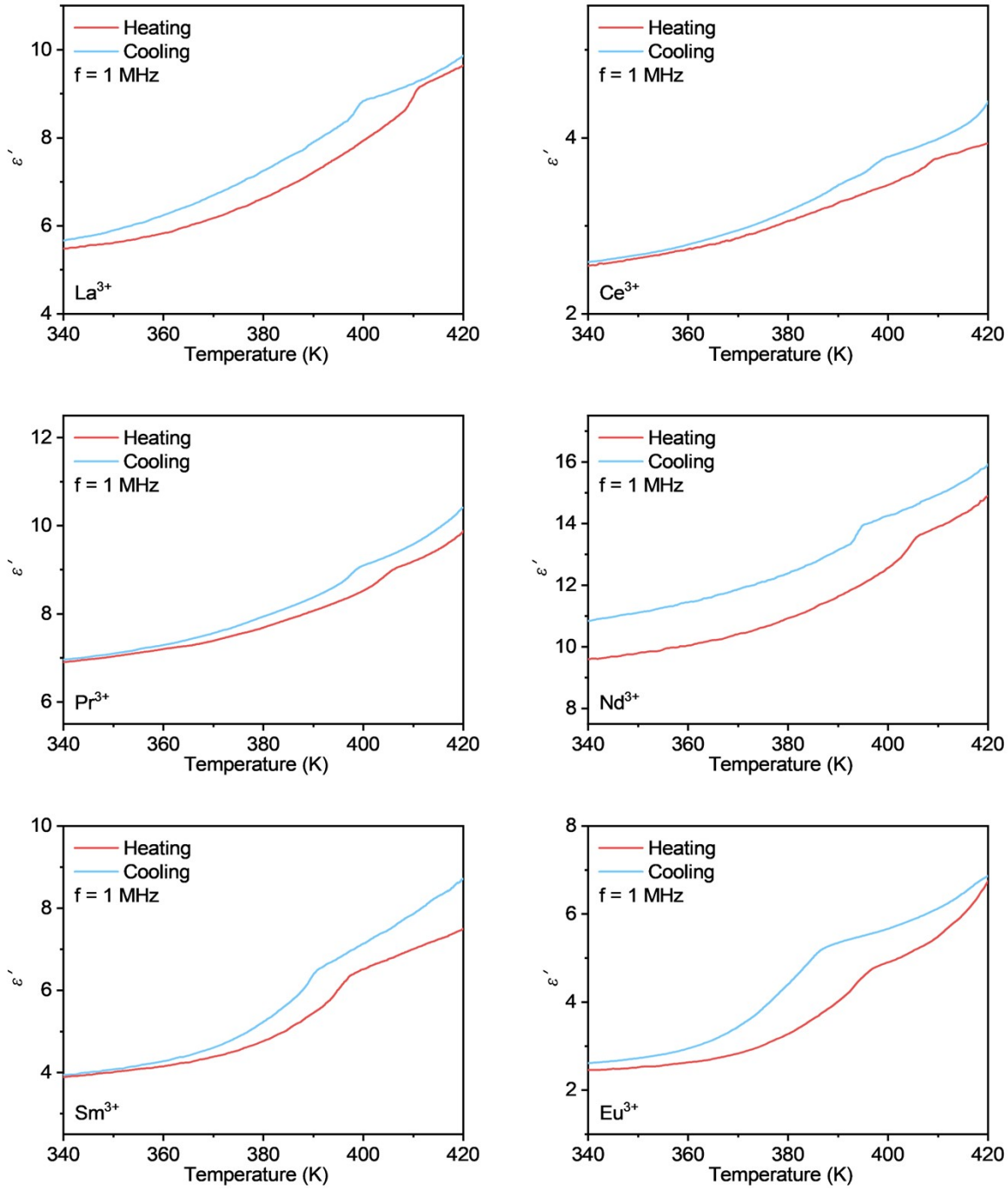

Fig. S4. The temperature-dependent ε' of $(DMSOX)_2LnCs(NO_3)_6$ at 1 MHz.

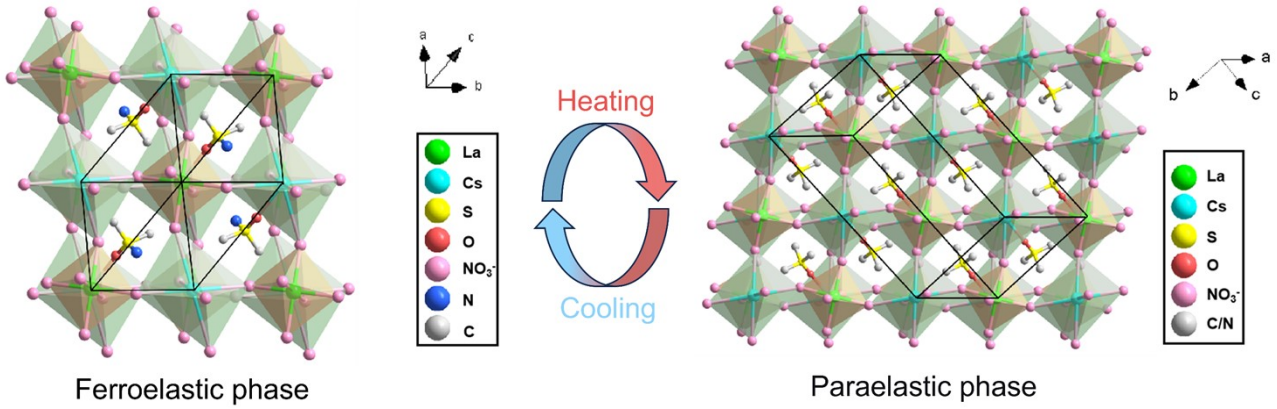

Fig. S5. The 3D perovskite cage of $(DMSOX)_2LaCs(NO_3)_6$ in the FP and PP.

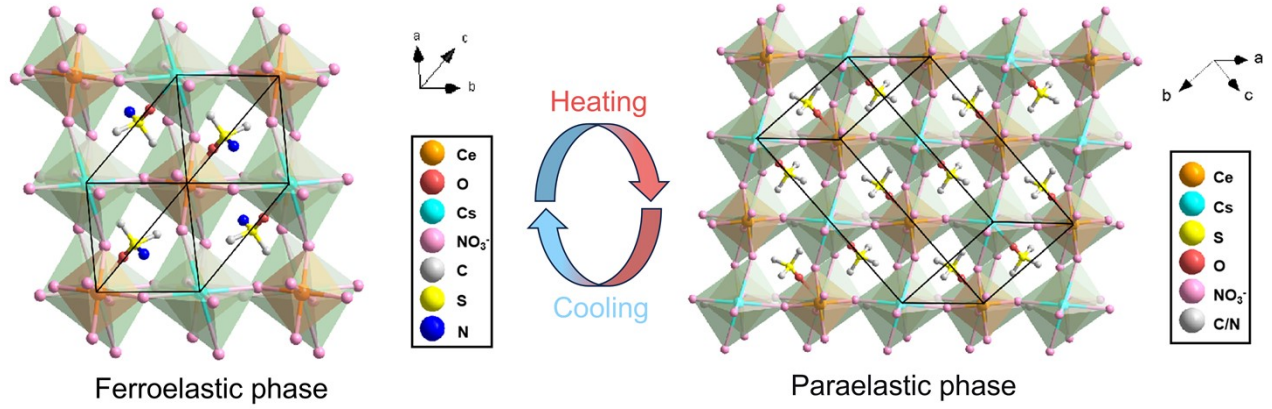

Fig. S6. The 3D perovskite cage of $(DMSOX)_2CeCs(NO_3)_6$ in the FP and PP.

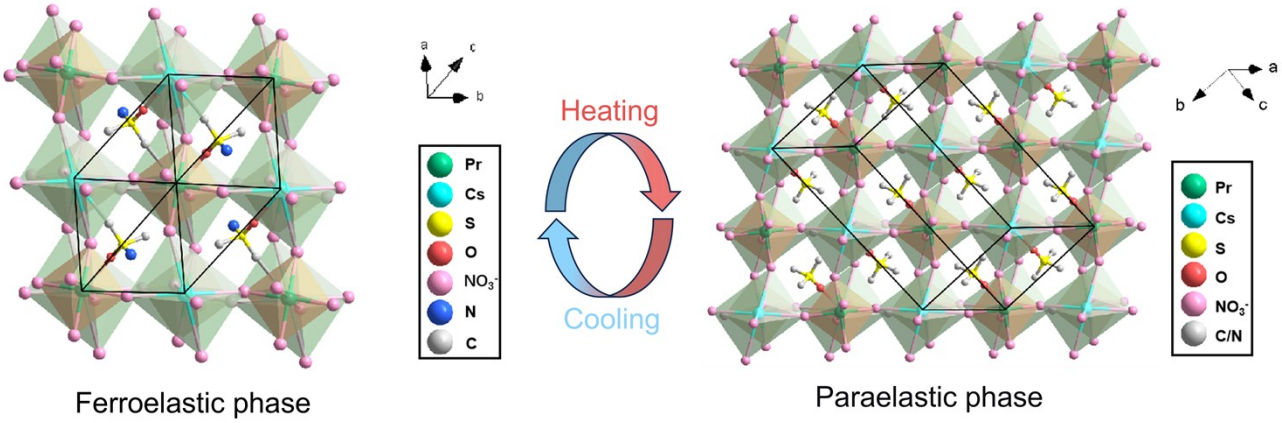

Fig. S7. The 3D perovskite cage of $(DMSOX)_2PrCs(NO_3)_6$ in the FP and PP.

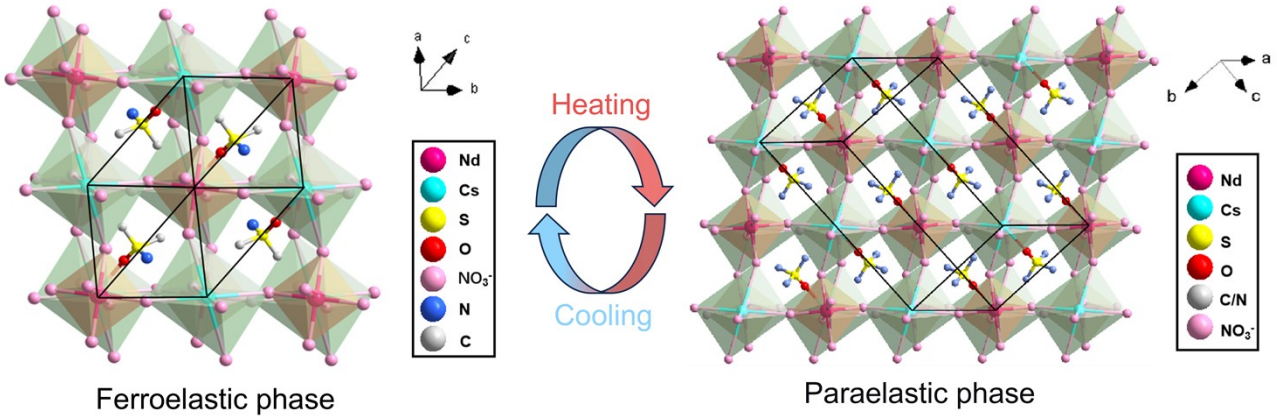

Fig. S8. The 3D perovskite cage of $(DMSOX)_2NdCs(NO_3)_6$ in the FP and PP.

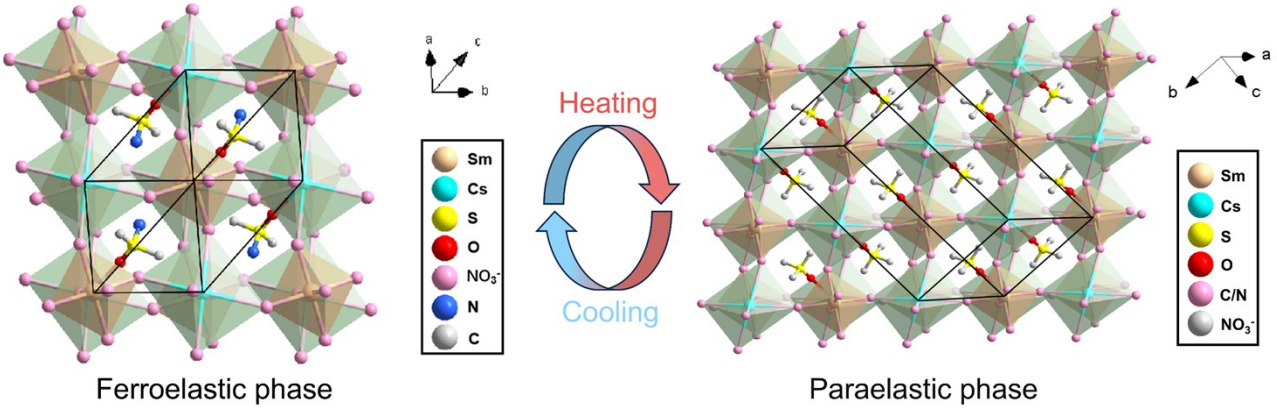

Fig. S9. The 3D perovskite cage of $(DMSOX)_2SmCs(NO_3)_6$ in the FP and PP.

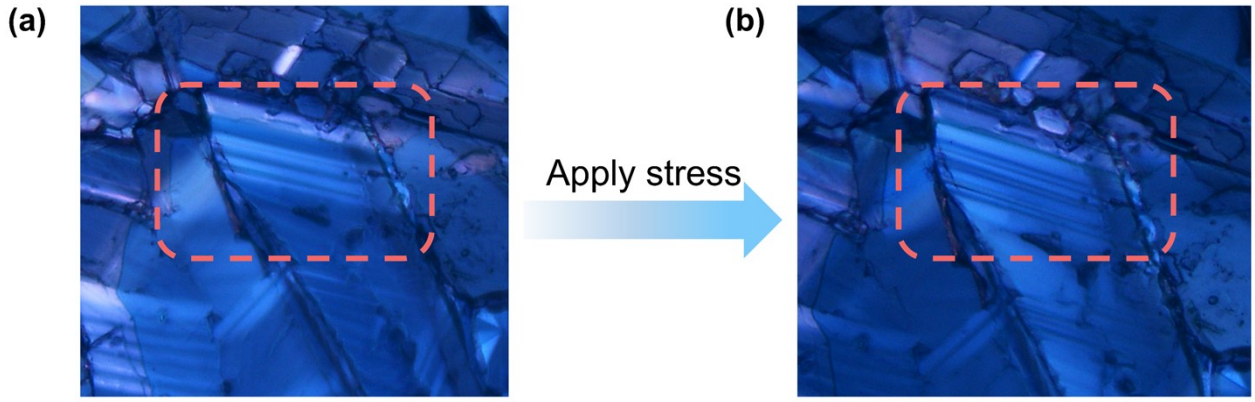

Fig. S10. (a-b) Stress-induced ferroelastic domain evolution in $(DMSOX)_2EuCs(NO_3)_6$ observed by a CX40P polarized light microscope.

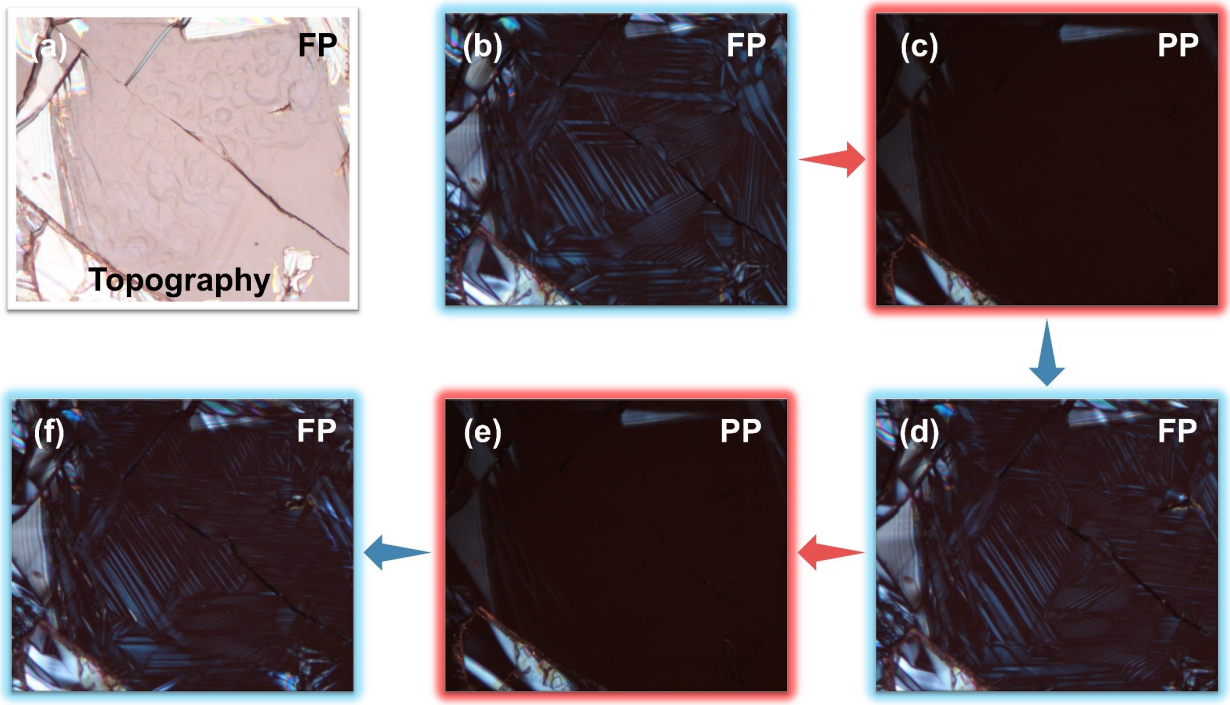

Fig. S11. (a) The topography of $(DMSOX)_2LaCs(NO_3)_6$ crystal in the FP. (b-f) Evolution of ferroelastic domain for $(DMSOX)_2LaCs(NO_3)_6$ between FP and PP.

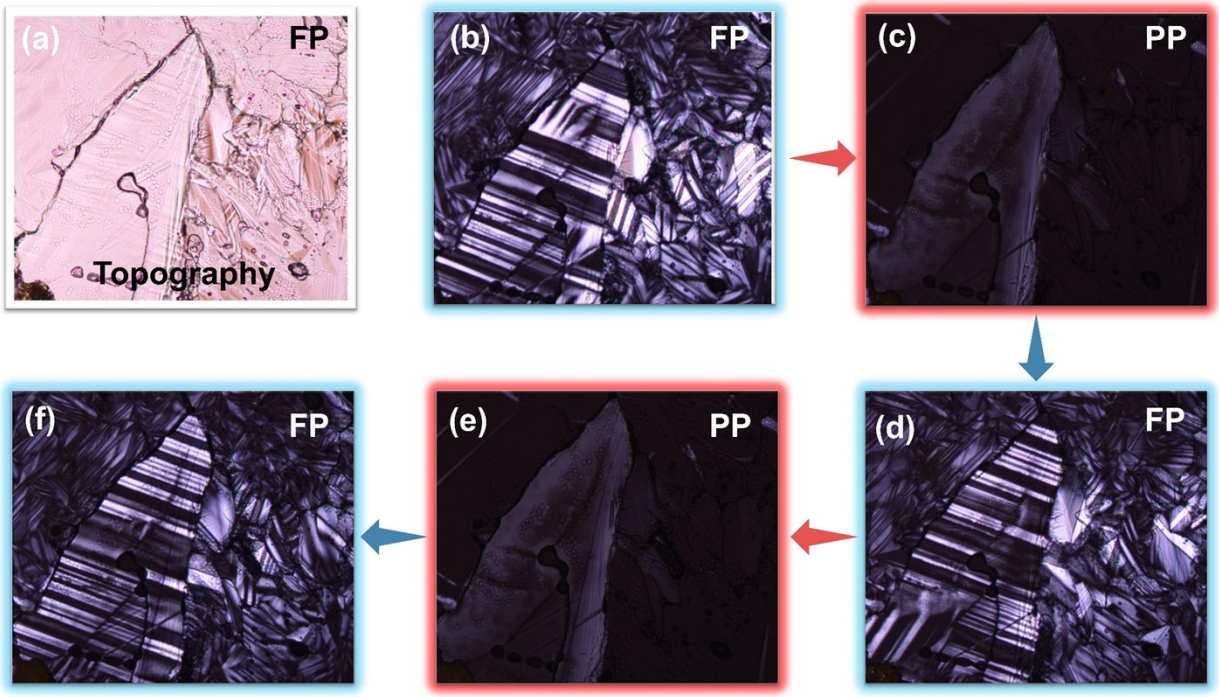

Fig. S12. (a) The topography of $(DMSOX)_2CeCs(NO_3)_6$ crystal in the FP. (b-f) Evolution of ferroelastic domain for $(DMSOX)_2CeCs(NO_3)_6$ between FP and PP.

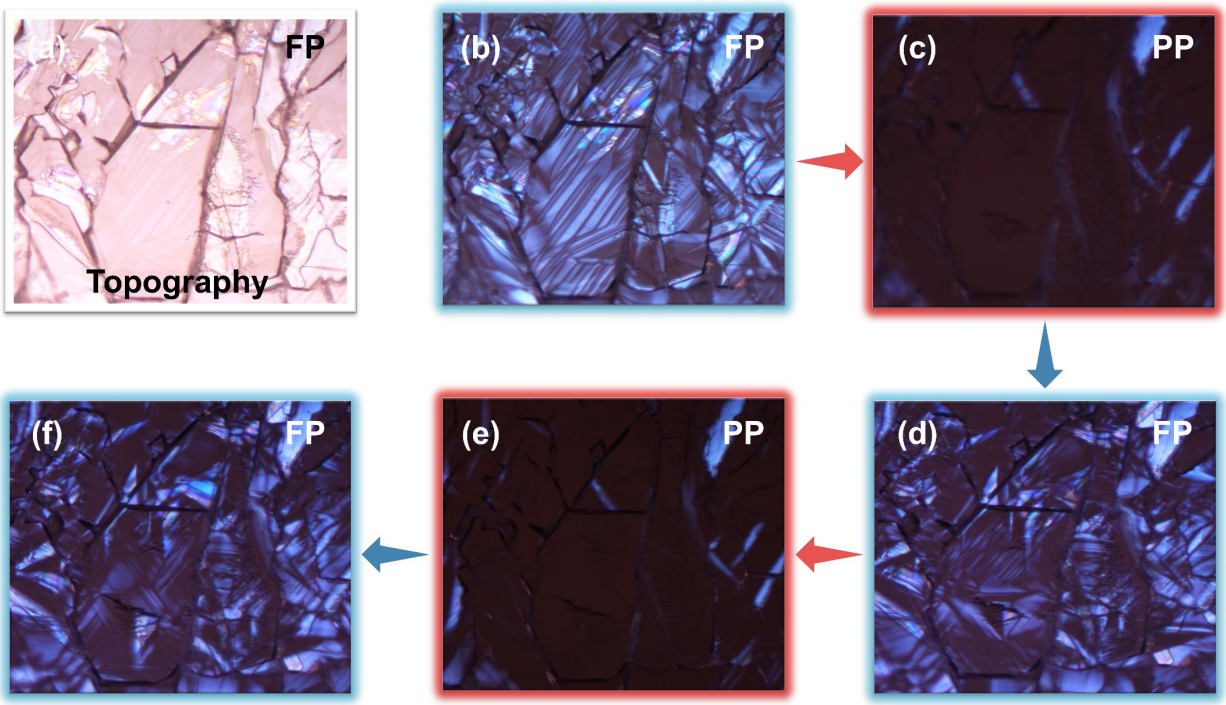

Fig. S13. (a) The topography of $(DMSOX)_2PrCs(NO_3)_6$ crystal in the FP. (b-f) Evolution of ferroelastic domain for $(DMSOX)_2PrCs(NO_3)_6$ between FP and PP.

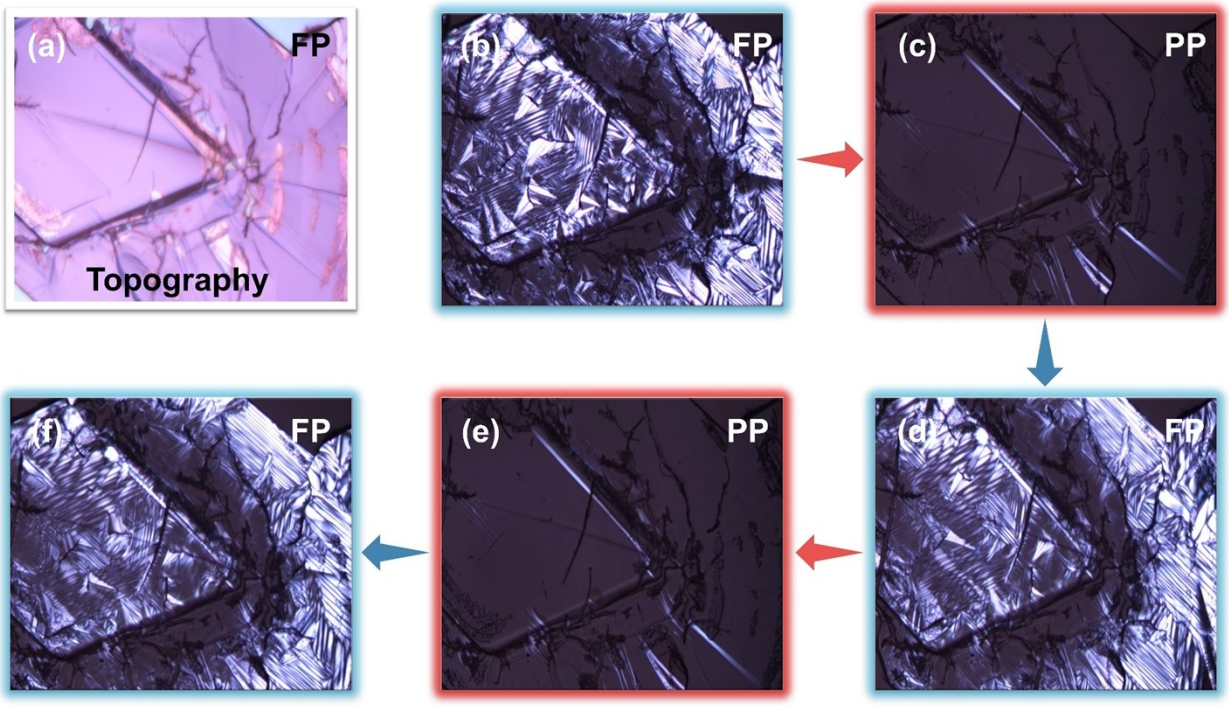

Fig. S14. (a) The topography of $(DMSOX)_2NdCs(NO_3)_6$ crystal in the FP. (b-f) Evolution of ferroelastic domain for $(DMSOX)_2NdCs(NO_3)_6$ between FP and PP.

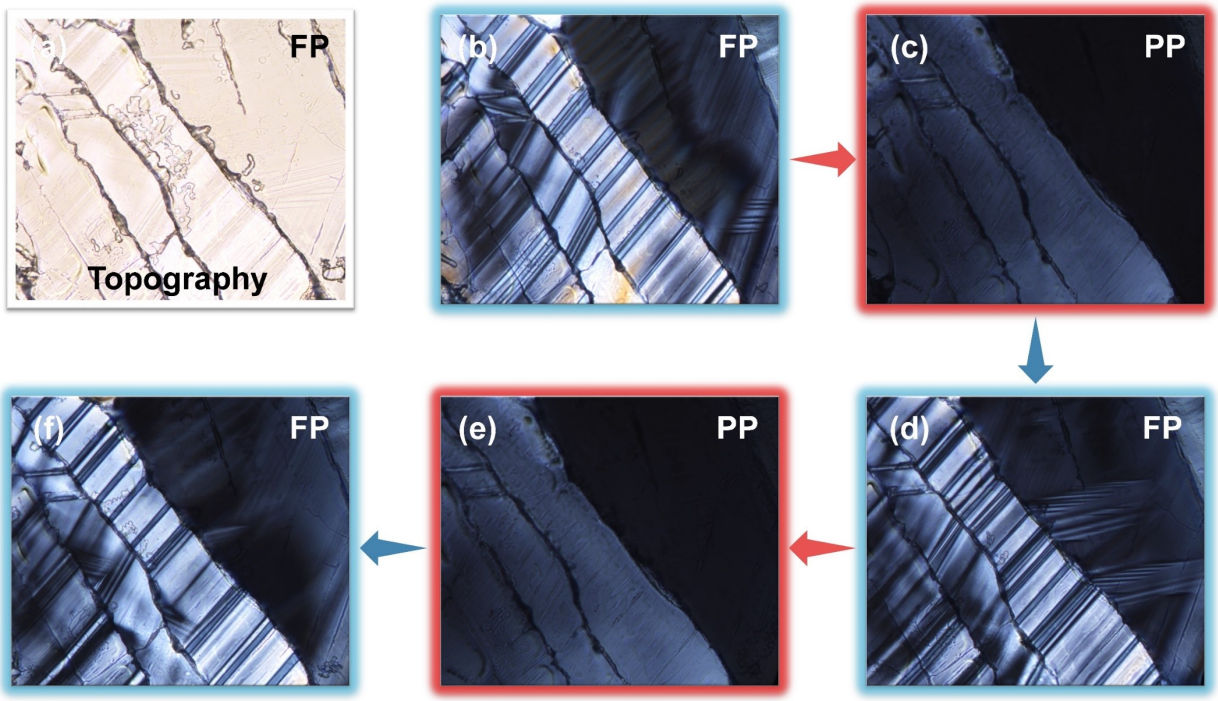

Fig. S15. (a) The topography of $(DMSOX)_2SmCs(NO_3)_6$ crystal in the FP. (b-f) Evolution of ferroelastic domain for $(DMSOX)_2SmCs(NO_3)_6$ between FP and PP.

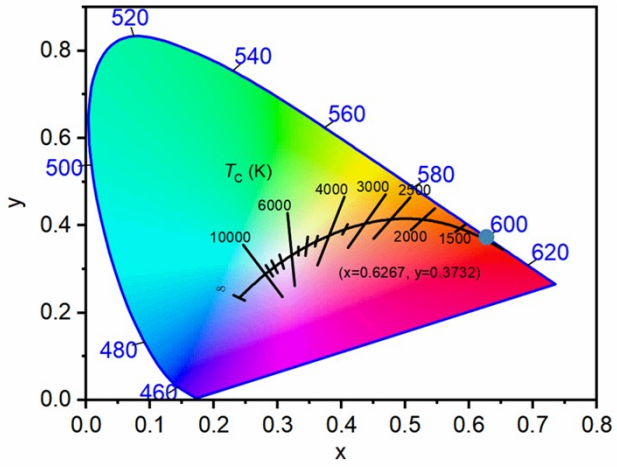

Fig. S16. The corresponding CIE chromaticity diagram of $(DMSOX)_2EuCs(NO_3)_6$.

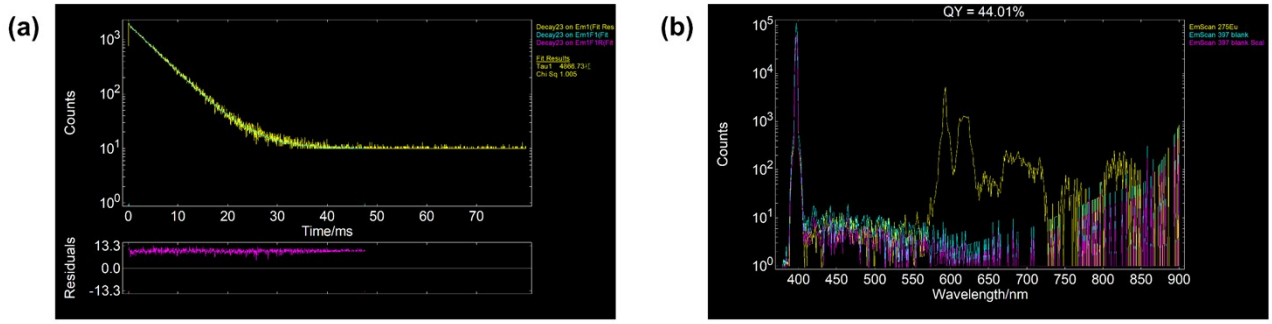

Fig. S17. The fluorescence lifetime of $(DMSOX)_2EuCs(NO_3)_6$ (a) and the quantum yields of $(DMSOX)_2EuCs(NO_3)_6$ (b).

Table S1. Comparison of key thermodynamic parameters for $(DMSOX)_2LnCs(NO_3)_6$ compounds.

	T_d (K)	T_C (K)	ΔS (J mol^{-1} K^{-1})	ΔH (kJ mol^{-1})	N
$(DMSOX)_2LaCs(NO_3)_6$	480	411.1	7.449	3.062	2.450
$(DMSOX)_2CeCs(NO_3)_6$	478	408.6	7.171	2.930	2.369
$(DMSOX)_2PrCs(NO_3)_6$	476	405.6	6.927	2.810	2.301
$(DMSOX)_2NdCs(NO_3)_6$	471	405.5	6.919	2.806	2.298
$(DMSOX)_2SmCs(NO_3)_6$	462	397.7	6.835	2.718	2.275
$(DMSOX)_2EuCs(NO_3)_6$	453	395.8	6.671	2.640	2.231

Table S2. Crystal data and structure refinements of $(DMSOX)_2LaCs(NO_3)_6$ at 300 K and 423 K.

Compound	$(DMSOX)_2LaCs(NO_3)_6$	
Temperature/K	300	423
Formula	$C_4H_{16}CsLaN_8O_{20}S_2$	$C_4H_{16}CsLaN_8O_{20}S_2$
Formula weight	832.19	832.19
Crystal system	triclinic	trigonal
Space group	$P\bar{1}$	$R\bar{3}$
a/Å	9.1970(19)	10.268(2)
b/Å	9.2214(19)	10.268(2)
c/Å	9.280(2)	21.566(4)
α/°	68.657(5)	90
β/°	63.620(5)	90
γ/°	67.868(5)	120.00(3)
Volume/Å^3	634.6(2)	1969.0(8)
Z	1	3
F(000)	400.0	1200.0
R_{int}	0.0656	0.1261
GOF	0.859	1.077
R_1	0.0219	0.0660
wR_2	0.0549	0.1999

Table S3. Crystal data and structure refinements of $(DMSOX)_2CeCs(NO_3)_6$ at 300 K and 423 K.

Compound	$(DMSOX)_2CeCs(NO_3)_6$	
Temperature/K	300	423
Formula	$C_4H_{16}CsCeN_8O_{20}S_2$	$C_4H_{16}CsCeN_8O_{20}S_2$
Formula weight	833.40	833.40
Crystal system	triclinic	trigonal
Space group	$P\bar{1}$	$R\bar{3}$
a/Å	9.184(3)	10.194
b/Å	9.218(3)	10.194
c/Å	9.246(3)	21.445
α/°	68.552(7)	90
β/°	63.731(6)	90
γ/°	67.834(7)	120
Volume/Å^3	631.2(3)	1930.1
Z	1	3
F(000)	401.0	1203.0
R_{int}	0.0880	0.0754
GOF	1.121	1.082
R_1	0.0308	0.0629
wR_2	0.0708	0.1952

Table S4. Crystal data and structure refinements of $(DMSOX)_2PrCs(NO_3)_6$ at 300 K and 423 K.

Compound	$(DMSOX)_2PrCs(NO_3)_6$	
Temperature/K	300	423
Formula	$C_4H_{16}CsPrN_8O_{20}S_2$	$C_4H_{16}CsPrN_8O_{20}S_2$
Formula weight	834.19	834.19
Crystal system	triclinic	trigonal
Space group	$P\bar{1}$	$R\bar{3}$
a/Å	9.1625(15)	10.176(2)
b/Å	9.1792(16)	10.176(2)
c/Å	9.2035(16)	21.443(4)
α/°	68.498(5)	90.00(3)
β/°	63.792(5)	90.00(3)
γ/°	67.680(5)	120.00(3)
Volume/Å^3	623.74(19)	1922.9(8)
Z	1	3
F(000)	402.0	1206.0
R_{int}	0.0403	0.0529
GOF	1.119	1.147
R_1	0.0189	0.0414
wR_2	0.0446	0.1137

Table S5. Crystal data and structure refinements of $(DMSOX)_2NdCs(NO_3)_6$ at 300 K and 423 K.

Compound	$(DMSOX)_2NdCs(NO_3)_6$	
Temperature/K	300	423
Formula	$C_4H_{16}CsNdN_8O_{20}S_2$	$C_4H_{16}CsNdN_8O_{20}S_2$
Formula weight	837.52	837.52
Crystal system	triclinic	trigonal
Space group	$P\bar{1}$	$R\bar{3}$
a/Å	9.128(3)	10.168(2)
b/Å	9.154(3)	10.168(2)
c/Å	9.162(2)	21.417(6)
α/°	68.549(7)	90
β/°	63.809(7)	90
γ/°	67.715(7)	120
Volume/Å^3	617.3(3)	1917.6(9)
Z	1	3
F(000)	403.0	1209.0
R_{int}	0.0492	0.0564
GOF	1.016	1.088
R_1	0.0217	0.0612
wR_2	0.0496	0.1672

Table S6. Crystal data and structure refinements of $(DMSOX)_2SmCs(NO_3)_6$ at 300 K and 423 K.

Compound	$(DMSOX)_2SmCs(NO_3)_6$	
Temperature/K	300	423
Formula	$C_4H_{16}CsSmN_8O_{20}S_2$	$C_4H_{16}CsSmN_8O_{20}S_2$
Formula weight	843.63	843.63
Crystal system	triclinic	trigonal
Space group	$P\bar{1}$	$R\bar{3}$
a/Å	9.1235(17)	10.156(2)
b/Å	9.1435(18)	10.156(2)
c/Å	9.1554(18)	21.412(4)
α/°	68.382(5)	90.00(3)
β/°	67.597(6)	90.00(3)
γ/°	63.872(5)	120.00(3)
Volume/Å^3	615.2(2)	1912.8(8)
Z	1	3
F(000)	405.0	1215.0
R_{int}	0.0523	0.0809
GOF	1.125	1.114
R_1	0.0214	0.0485
wR_2	0.0508	0.1374

Table S7. Crystal data and structure refinements of $(DMSOX)_2EuCs(NO_3)_6$ at 300 K and 423 K.

Compound	$(DMSOX)_2EuCs(NO_3)_6$	
Temperature/K	300	423
Formula	$C_4H_{16}CsEuN_8O_{20}S_2$	$C_4H_{16}CsEuN_8O_{20}S_2$
Formula weight	845.24	845.24
Crystal system	triclinic	trigonal
Space group	$P\bar{1}$	$R\bar{3}$
a/Å	9.120(6)	10.127
b/Å	9.139(6)	10.127
c/Å	9.147(6)	21.379
α/°	68.426(15)	90
β/°	67.63(2)	90
γ/°	63.85(2)	120
Volume/Å^3	614.2(7)	1898.8
Z	1	3
F(000)	406.0	1218.0
R_{int}	0.1123	0.1053
GOF	1.059	1.052
R_1	0.0351	0.0443
wR_2	0.0868	0.1099

Table S8. The ionic radius of trivalent rare-earth ions with 12 coordination numbers.

Ln^{3+}	Ionic radius/Å (N = 12)
La^{3+}	1.50
Ce^{3+}	1.48
Pr^{3+}	1.46
Nd^{3+}	1.45
Sm^{3+}	1.43
Eu^{3+}	1.42

Table S9. Hydrogen bonding data for $(DMSOX)_2LaCs(NO_3)_6$ at 300 K.

D–H···A	d(D–H)/Å	d(H–A)/Å	d(D–A)/Å	D–H–A/°
N3–H3A···O8$^{\#1}$	0.86	2.60	3.424(4)	161.3
N3–H3B···O3$^{\#2}$	0.86	2.61	3.345(5)	144.0
C1–H1A···O3$^{\#1}$	0.96	2.59	3.332(5)	134.3
C1–H1B···O6$^{\#3}$	0.96	2.49	3.318(5)	144.4
C1–H1C···O5$^{\#4}$	0.96	2.44	3.370(5)	164.0
C1–H1C···O7$^{\#4}$	0.96	2.61	3.371(6)	136.8
C2–H2B···O7$^{\#3}$	0.96	2.57	3.242(6)	127.3
C2–H2C···O8$^{\#5}$	0.96	2.50	3.357(5)	148.3
C2–H2C···O10	0.96	2.55	3.334(5)	139.5

Symmetry transformations used to generate equivalent atoms: #1: 1+X, +Y, -1+Z; #2: 2-X, 1-Y, 1-Z; #3: 2-X, -Y, 1-Z; #4: 1+X, +Y, +Z; #5: 1-X, 1-Y, 1-Z.

Table S10 Hydrogen bonding data for $(DMSOX)_2CeCs(NO_3)_6$ at 300 K.

D–H···A	d(D–H)/Å	d(H–A)/Å	d(D–A)/Å	D–H–A/°
C1–H1A···O3	0.96	2.61	3.334(5)	132.2
C1–H1B···O6$^{\#1}$	0.96	2.46	3.312(5)	147.4
C1–H1C···O5$^{\#2}$	0.96	2.44	3.383(5)	165.8
C1–H1C···O7$^{\#2}$	0.96	2.61	3.375(6)	136.3
C2–H2B···O7$^{\#1}$	0.96	2.58	3.237(5)	125.6
C2–H2C···O4$^{\#3}$	0.96	2.50	3.360(5)	148.8
C2–H2C···O10$^{\#4}$	0.96	2.54	3.335(5)	139.8
N3–H3A···O4	0.86	2.60	3.417(4)	160.3
N3–H3B···O3$^{\#2}$	0.86	2.61	3.349(5)	144.0

Symmetry transformations used to generate equivalent atoms: #1: +X, -1+Y, 1+Z; #2: 1-X, 1-Y, 1-Z; #3: -X, 1-Y, 1-Z; #4: -1+X, +Y, 1+Z.

Table S11 Hydrogen bonding data for $(DMSOX)_2PrCs(NO_3)_6$ at 300 K.

D–H···A	d(D–H)/Å	d(H–A)/Å	d(D–A)/Å	D–H–A/°
N3–H3A···O4	0.86	2.58	3.401(4)	160.2
N3–H3B···O3$^{\#1}$	0.86	2.58	3.315(4)	143.9
C1–H1A···O6$^{\#2}$	0.96	2.47	3.312(4)	145.8
C1–H1B···O10$^{\#1}$	0.96	2.45	3.381(4)	163.2
C1–H1B···O2$^{\#1}$	0.96	2.59	3.357(5)	136.6
C1–H1C···O3	0.96	2.58	3.323(4)	134.3
C2–H2A···O4$^{\#3}$	0.96	2.49	3.346(4)	148.7
C2–H2A···O8$^{\#4}$	0.96	2.53	3.328(4)	140.2
C2–H2C···O2$^{\#2}$	0.96	2.53	3.230(4)	129.8

Symmetry transformations used to generate equivalent atoms: #1: 1-X, 1-Y, 1-Z; #2: +X, -1+Y, 1+Z; #3: -X, 1-Y, 1-Z; #4: -1+X, +Y, 1+Z.

Table S12 Hydrogen bonding data for $(DMSOX)_2NdCs(NO_3)_6$ at 300 K.

D–H···A	d(D–H)/Å	d(H–A)/Å	d(D–A)/Å	D–H–A/°
N4–H4A···O5	0.86	2.56	3.382(4)	159.8
N4–H4B···O7$^{\#1}$	0.86	2.57	3.302(5)	144.0
C2–H2A···O1	0.96	2.65	3.427(4)	138.0
C2–H2A···O7	0.96	2.56	3.313(4)	135.8
C2–H2B···O6$^{\#2}$	0.96	2.45	3.376(5)	161.5
C2–H2B···O8$^{\#2}$	0.96	2.58	3.354(5)	137.3
C2–H2C···O2$^{\#3}$	0.96	2.48	3.312(4)	144.7
C3–H3A···O8$^{\#3}$	0.96	2.50	3.218(5)	131.1
C3–H3C···O3$^{\#4}$	0.96	2.51	3.310(4)	140.4

Symmetry transformations used to generate equivalent atoms: #1: 1-X, 1-Y, -Z; #2: +X, +Y, -1+Z; #3: 1-X, 2-Y, -Z; #4: 1+X, +Y, -1+Z; #5: 2-X, 1-Y, -Z.

Table S13 Hydrogen bonding data for $(DMSOX)_2SmCs(NO_3)_6$ at 300 K.

D–H···A	d(D–H)/Å	d(H–A)/Å	d(D–A)/Å	D–H–A/°
N4–H4A···O5	0.86	2.56	3.380(3)	159.1
N4–H4B···O7$^{\#1}$	0.86	2.57	3.303(4)	144.4
C1–H1A···O7	0.96	2.57	3.308(4)	134.1
C1–H1B···O3$^{\#2}$	0.96	2.47	3.312(4)	147.0
C1–H1C···O6$^{\#1}$	0.96	2.46	3.390(4)	163.0
C1–H1C···O8$^{\#1}$	0.96	2.58	3.353(4)	137.2
C2–H2B···O8$^{\#2}$	0.96	2.52	3.227(4)	130.2
C2–H2C···O4$^{\#3}$	0.96	2.52	3.316(4)	140.7
C2–H2C···O5$^{\#4}$	0.96	2.48	3.339(4)	149.4

Symmetry transformations used to generate equivalent atoms: #1: 1-X, 1-Y, 1-Z; #2: +X, -1+Y, 1+Z; #3: 1+X, -1+Y, +Z; #4: 2-X, 1-Y, 1-Z.

Table S14 Hydrogen bonding data for $(DMSOX)_2EuCs(NO_3)_6$ at 300 K

D–H···A	d(D–H)/Å	d(H–A)/Å	d(D–A)/Å	D–H–A/°
N4–H4A···O3$^{\#1}$	0.86	2.56	3.376(7)	158.8
N4–H4B···O7$^{\#2}$	0.86	2.56	3.297(8)	144.6
C1–H1A···O7$^{\#3}$	0.96	2.62	3.305(8)	128.7
C1–H1B···O5$^{\#4}$	0.96	2.43	3.313(8)	152.0
C1–H1C···O$^{6\#2}$	0.96	2.43	3.374(8)	169.4
C1–H1C···O8$^{\#2}$	0.96	2.59	3.342(9)	135.7
C2–H2B···O8$^{\#4}$	0.96	2.47	3.221(9)	135.3
C2–H2C···O2	0.96	2.52	3.318(8)	140.7
C2–H2C···O3	0.96	2.49	3.342(8)	148.1

Symmetry transformations used to generate equivalent atoms: #1: 1-X, 2-Y, 1-Z; #2: 1-X, 1-Y, 1-Z; #3: -1+X, 1+Y, +Z; #4: -1+X, +Y, 1+Z.